 doi:10.20944/preprints201810.0574.v1

Pep-1&Borneol-bifunctionalized carmustin-loaded micelles enhance anti-glioma efficacy through tumor targeting and BBB penetrating

Xiaoyuan Guo[1], Guojian Wu[1], Yue Qin[2], Hong Wang[1], Ding Qu[2,*], Lukui Chen[1,*]

[1] Department of Neurosurgery, School of Medicine, Zhongda Hospital, Southeast University, Nanjing 210009, China; guoxiaoyuan@gmail.com (X.G.); jianjian0513@126.com (G.W.); xnwanghong@126.com (H.W.)

[2] Affiliated Hospital of Integrated Traditional Chinese and Western Medicine, Nanjing University of Chinese Medicine, Nanjing 210028, China; 270964569@qq.com (Y.Q.)

[*]Correspondence: 101011658@seu.edu.cn (L.C.); quding@jsatcm.com (D.Q.)

Tel: +86 25 83262271 (L.C.); +86 25 85232155 (D.Q.); Fax: 86-25-83272011 (L.C.)

Preprints (www.preprints.org) | NOT PEER-REVIEWED | Posted: 24 October 2018 doi:10.20944/preprints201810.0574.v1

Pep-1&Borneol-bifunctionalized carmustin-loaded micelles enhance anti-glioma efficacy through tumor targeting and BBB penetrating

Abstract: Tumor-targeting and blood-brain barrier (BBB)-penetrating are highly desirable for the treatment of glioma. In this study, we developed Pep-1&borneol-bifunctionalized carmustin-loaded micelles (Pep-1/Bor/CMS-M) capable of targeting to IL-13 receptor-overexpressed glioma and penetrating the brain microvascular endothelial cells-associated physiologic barriers. Pep-1/Bor/CMS-M were nearly spherical particles with a dimeter of 32.6 ± 1.1 nm and zeta potential of -21.3 ± 3.1 mV. Carmustine (CMS) released from Pep-1/Bor/CMS-M in pH 7.4 was significantly faster than in acidic environments. In human glioma BT325 cellular studies, Pep-1/Bor/CMS-M remarkably increased the cytotoxicity, notably improved the internalization and effectively induced the cell apoptosis. Likewise, in human brain microvascular endothelial cells (HBMEC) cells, Pep-1/Bor/CMS-M obviously promoted the cellular uptake, rapidly decreased the transepithelial electrical resistance (TEER) and thereby of enhancing the ability of penetration. In orthotopic Luc-BT325 glioma tumor-bearing nude mouse models, the stronger fluorescence signal and longer retention were observed in brain tissues compared with other controls, after single administration of DiD-labelled Pep-1/Bor/M (DiD/Pep-1/Bor/M). Importantly, Pep-1/Bor/CMS-M displayed the strongest inhibition of tumor growth, the longest survival period and low systemic toxicity in treating orthotopic glioma tumor-bearing nude mice. Simultaneous functionalization of Pep-1 and borneol offers a novel strategy for designing CMS-based nanomedicine and precisely treating glioma.

Keywords: carmustine-loaded micelle; brain targeting; borneol; IL-13 receptor; BBB

Preprints (www.preprints.org) | NOT PEER-REVIEWED | Posted: 24 October 2018 doi:10.20944/preprints201810.0574.v1

1. Introduction

Glioma is the most common primary intracranial malignancy, accounting for 50% to 60% of brain tumors in humans [1]. It is highly malignant, aggressive, has a poor prognosis, and poses a serious challenge to human health. Carmustine (CMS) is a cell-specific nitrosourea alkylating agent, which can inhibit DNA repair and RNA synthesis in glioma cells. CMS is the first-line drug for clinical treatment of glioma, as it is capable of penetrating the blood-brain barrier (BBB) due to its high lipophilicity [2,3]. Clinical reports, however, have revealed the following limitations of using CMS: 1. *in vivo* half-life of 15 ~ 30 min, which makes it difficult to maintain effective concentrations in tumor sites or cells; 2. no selectivity for tumor cells, resulting in a large number of secondary effects, such as blood toxicity, bone marrow suppression, liver and kidney injury, among others; and 3. the retention in the brain is not long enough to exert the sustained anticancer efficacy. These adverse reactions greatly reduce the patient's compliance to treatment and their quality of life [4,5].

Polymer micelles with a "shell-core" structure are self-assembled by suitable polymer materials to carry insoluble drugs in the aqueous phase. The use of these structures for drug delivery not only offer the advantage of physically blocking direct contact between cytotoxic drugs and normal tissues but can also provide a way to penetrate the BBB, by reducing the efflux of vascular endothelial cells in brain tissues [6]. In addition, polymer micelles can significantly improve the solubility and bioavailability of hydrophobic drugs and avoid their degradation by a variety of enzymes *in vivo*. For example, when using paclitaxel chitosan [7], paclitaxel NK-105 [8], and vitamin E TPGS [9] micelles, the solubility of insoluble drugs in the aqueous phase was greatly increased, and their stability improved to a certain extent.

The BBB is a unique physiological barrier that protects the homeostasis of the brain's own microenvironment and blocks the distribution of approximately 100% of high molecular weight drugs and over 98% of low molecular weight drugs into the brain. Therefore, brain-targeted drug delivery systems that facilitate the passage through the BBB have become a hot research topic [10-12].

Borneol is commonly used in traditional Chinese medicine to help other

 doi:10.20944/preprints201810.0574.v1

components enter the brain. Modern medicine has proved that borneol can facilitate the opening of the BBB and enhance the permeation and distribution of drugs into the brain in a reversible way. Huang et al. tested the distribution of borneol after a single injection and confirmed that its localization in the brain tissue was much higher than in other tissues [13]. Zheng et al. modified borneol with nano-structured lipid carriers, significantly improving the delivery efficiency of drugs in the brain [14]. These reports suggest that using borneol as a BBB permeation-promoting functional group effectively improves the intracerebral delivery of nanodrugs. However, nanoparticles simply modified with Bor has limited improvement on drug retention in the brain. Therefore, it is urgent to seek a combinational strategy enabling delivery system recognize glioma efficiently, have affinity to tumor highly, as well as penetrate the BBB readily [15].

Gliomas are usually infiltrative, without definite boundaries, and are difficult to remove completely by traditional surgery. Nonselective radiotherapy and chemotherapy can easily cause irreversible damage to normal brain tissue [16,17]. Interleukin-13 receptor (IL-13R) is a highly expressed specific molecular marker on the surface of glioma cells and is positively correlated with glioma malignancy. It has been reported that IL-13R-expressed cells in malignant glioma is as high as 30,000 cells, and that in multiform glioblastoma is as high as 500,000 cells [18,19]. Previous papers reported a short peptide protein Pep-1, which can effectively penetrate the blood-brain tumor barrier and demonstrate high affinity for a subtype of IL-13R (IL-13R-α2) [20,21]. They constructed a Pep-1 modified nanoparticle that can carry enough drugs into the tumor tissue, demonstrating the advantages of targeted therapy for glioma.

In this study, we used borneol-conjugated distearoyl phosphoethanolamine-polyethylene glycol (DSPE-PEG-Bor) to promote BBB-permeation, Pep-1-modified DSPE-PEG (DSPE-PEG-Pep-1) to target glioma cells, and DSPE-PEG and dioleoyl phosphoethanolamine (DOPE) as carrier materials. CMS was assembled into micellar drug delivery system (Pep-1/Bor/CMS-M) by a simple preparation process. This system is capable of penetrating BBB, and of actively targeting glioma cells, which increases accumulation of CMS in glioma, thereby circumventing its limitations, i.e., short half-life, poor retention and systemic toxicity. Additionally, our system was

Preprints (www.preprints.org) | NOT PEER-REVIEWED | Posted: 24 October 2018 doi:10.20944/preprints201810.0574.v1

capable of rapidly releasing the drug in an acidic environment due to the pH-sensitive property of DOPE [22]. Here, we focus on the preparation and characterization of micelles, their biological effects on tumor cells and BBB endothelial cells, and their distribution and anticancer efficacy towards orthotopic glioma models, to verify the effectiveness of the design, and to provide a new solution for the precise delivery of drugs to the glioma region.

2. Results and discussion

2.1 Characterizations of micelles

As shown in Table 1, CMS-M micelles exhibit a particle size of about 27 nm with a polydispersity index of less than 0.1, and a medium negative charge of -22.9 ± 1.1 mV. The encapsulation efficiency of CMS was higher than 95%, and its drug loading capacity was higher than 3%. The modification with borneol did not significantly change the pharmaceutical properties of the micelles, and the modification with Pep-1 exhibited no influence on the major physicochemical properties of the micelles. As shown in Figure 1A, the particle size of Pep-1/Bor/CMS-M was mainly distributed near 30 nm, and the morphology was nearly round. Compared with the TEM images of CMS-M or Bor/CMS-M, the functional modifications in Pep-1/Bor/CMS-M did not affect the basic shape of the micelles (Figure S1). In order to investigate the pH-stability of micelles, the particle size and zeta potential of Pep-1/Bor/CMS-M were monitored after incubation with PBS with different pH values. As shown in Figure 1B, the surface characteristics did not change obviously at pH values ranging from 8.0 to 6.5, however, both average size and surface charge at pH 2.0 were significantly increased compared with that at pH 7.4, suggesting that micelles were not stable under strongly acidic environment. To determine the optimal mass ratio of functional groups, the influence of weight ratios of DSPE-PEG-Bor and DSPE-PEG-Pep-1 on particle size investigated in Figure 1C and 1D. It was found that 5% (wt%) of DSPE-PEG-Bor and 10% (wt%) DSPE-PEG-Pep-1 nearly did not result in an obviously change in particle size, therefore, such feeding ratio was used in the following experiments. As shown in Figure 1E, we investigated the effect of different modifiers on drug release. The results showed that

Preprints (www.preprints.org) | NOT PEER-REVIEWED | Posted: 24 October 2018 doi:10.20944/preprints201810.0574.v1

in a pH 7.4 environment, all the micelles released their payloads with first-order release characteristics, and the 48 h-cumulative release ranged from 50% to 60% without statistical difference. However, the release profile of Pep-1/Bor/CMS-M showed significant differences in various pH environments. The 48 h-cumulative release of CMS varied considerably at pH 5.0 and pH 6.5, (76.8% and 62.3%, respectively, Figure 1F). This accelerated release of Pep-1/Bor/CMS-M under mildly acidic environment is helpful to killing tumor cells. According to previous reports, the characteristics of DOPE are involved with the pH-responsive release [23].

Table 1. Characterization of various types of micelles (n = 3).

Formulation	Size (nm)	PDI	Zeta (mV)	EE (%)	LE (%)
CMS-M	27.5 ± 0.8	0.084 ± 0.002	-22.9 ± 1.1	96.3 ± 2.2	3.3 ± 0.2
Bor/CMS-M	30.1 ± 1.8	0.102 ± 0.001	-19.3 ± 2.7	94.5 ± 3.9	3.1 ± 0.1
Pep-1/Bor/CMS-M	32.6 ± 1.1	0.113 ± 0.001	-21.3 ± 3.1	95.5 ± 1.4	3.4 ± 0.1

Preprints (www.preprints.org) | NOT PEER-REVIEWED | Posted: 24 October 2018 doi:10.20944/preprints201810.0574.v1

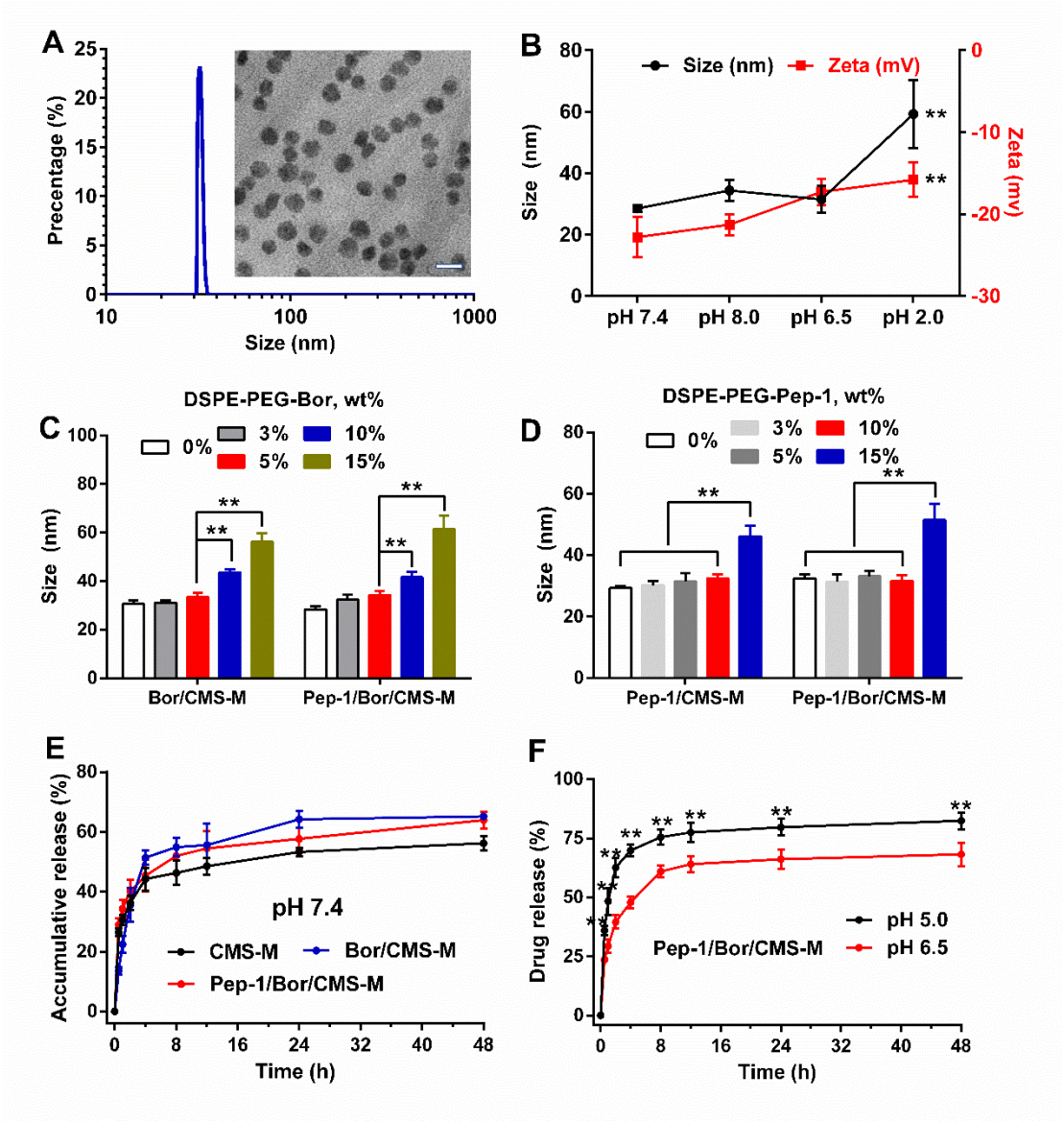

Figure 1. Characterizations of micelles. (A) Particle size distribution of Pep-1/Bor/CMS-M and its morphology in pH 7.4 (inset). (B) Particle size and zeta potential of Pep-1/Bor/CMS-M at different pH values. $^{**}P < 0.01$ vs corresponding result at pH 7.4 , $n = 4$, data are shown in mean ± SD. (C) Particle size of Bor/CMS-M and Pep-1/Bor/CMS-M with different weight ratio of DSPE-PEG-Bor. $^{**}P < 0.01$, $n = 4$, data are shown in mean ± SD. (D) Particle size of Pep-1/CMS-M and Pep-1/Bor/CMS-M with different weight ratio of DSPE-PEG-Pep-1. $^{**}P < 0.01$, $n = 4$, data are shown in mean ± SD. (E) Drug release profile of various types of micelles in pH 7.4 within 48 h. $n = 4$, data are shown in mean ± SD. (F) Drug release profile of Pep-1/Bor/CMS-M in different pH environments within 48 h. $^{**}P < 0.01$ vs pH 6.5 at corresponding time intervals, $n = 4$, data are shown in mean ± SD.

Preprints (www.preprints.org) | NOT PEER-REVIEWED | Posted: 24 October 2018 doi:10.20944/preprints201810.0574.v1

2.2 Influence of micelles on cancer cells

We investigated the effects of micelles on BT325 cellular behavior, including cell proliferation, cellular uptake, uptake mechanism, and apoptosis induction. As shown in Figure 2A, three types of micelles showed significant cytotoxicity compared to the free drug when the concentration of CMS was higher than 1 μg/mL. In addition, Pep-1/Bor/CMS-M inhibited BT325 cell proliferation more effectively than Bor/CMS-M, probably because of enhanced internalization through IL-13 receptor-mediated endocytosis. There were no significant differences between Bor/CMS-M and CMS-M in anticancer effect *in vitro*, suggesting that borneol modification did not contribute to increased cytotoxicity. In addition, we used C6 as a green fluorescent probe to evaluate cellular uptake of the different micelles by the cancer cells. As shown in Figure 2B, the cellular uptake of micelles was significantly higher than that of the free C6 group, suggesting that the lipid-based micelles were preferentially endocytosed. Compared to CMS-M, Bor/CMS-M entered the cells more easily, which is probably related to a borneol-based enhancement on membrane permeability. The internalization of Pep-1/Bor/CMS-M was further improved, reflecting the advantages of simultaneous functional modifications with borneol and Pep-1.

To explore the mechanism of cellular uptake, several classical uptake inhibitors were used. As shown in Figure 2C, the intracellular intensity of the micelles decreased significantly at low temperature, suggesting that micelles entered cells in an energy-dependent manner. Sucrose, a specific inhibitor of the clathrin-mediated endocytosis pathway, also significantly interfered with micelle internalization, suggesting that the clathrin-mediated pathway was involved with the endocytosis of micelles. More important, the cellular uptake of Pep-1/Bor/CMS-M decreased significantly under the competitive inhibition of free IL-13, indicating that Pep-1/Bor/CMS-M micelles entered the cell through the clathrin- and IL-13 receptor-mediated pathways in an energy-dependent manner. Finally, the effects of the different functional modification of the micelles on apoptosis induction were evaluated. As shown in Figure 2D, various formulations induce cancer cell apoptosis in a concentration-dependent manner. When the concentration of CMS was 2 μg/mL, Bor/CMS-M induced apoptosis in 60% BT325

Preprints (www.preprints.org) | NOT PEER-REVIEWED | Posted: 24 October 2018 doi:10.20944/preprints201810.0574.v1

cells, which was significantly higher than free drug did. When further modified with Pep-1, the apoptosis rate of Pep-1/Bor/CMS-M increased to nearly 80%, which might be related to an increase in cell uptake and enhanced stability of CMS after micelle encapsulation.

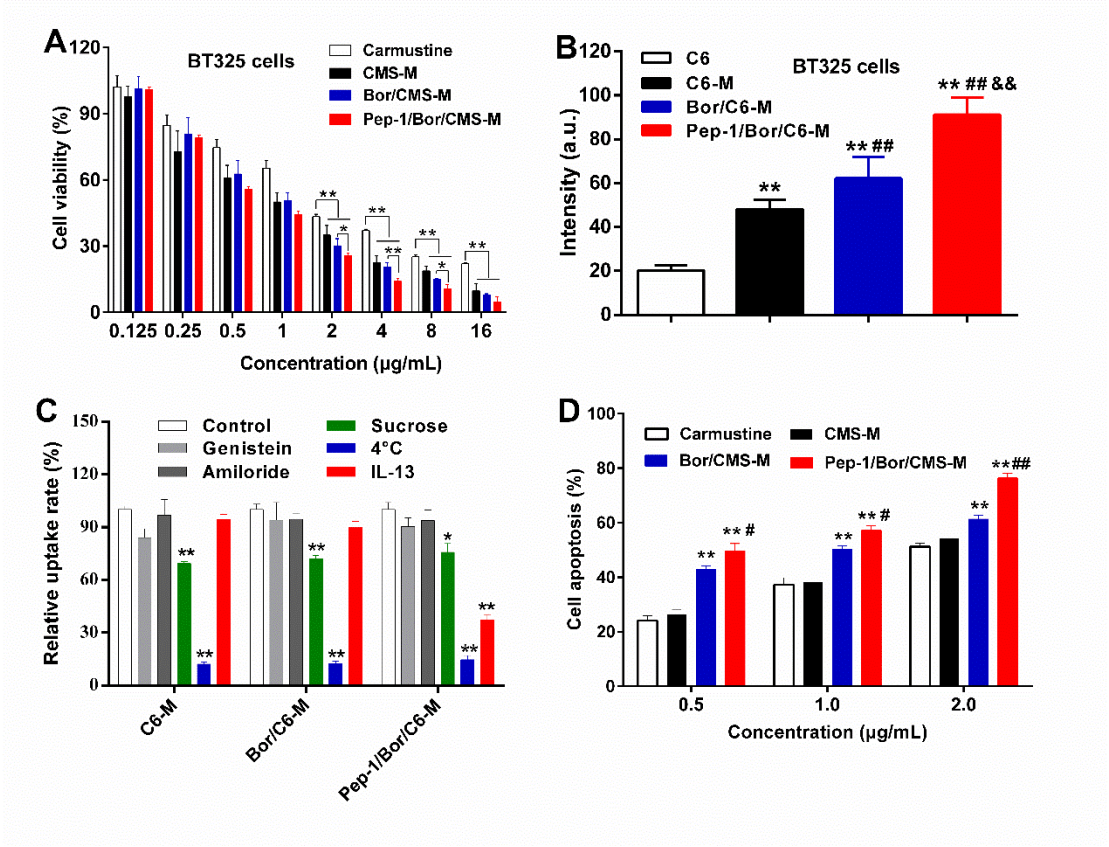

Figure 2. Influences of micelles on BT325 cells. (A) Antiproliferative effect of different micelles against BT325 cells. $^{**}P < 0.01$, $n = 6$, data are shown in mean ± SD. (B) Cellular uptake of micelles on BT325 cells. $^{**}P < 0.01$ vs CMS, $^{\#\#}P < 0.01$ vs C6-M, $^{\&\&}P < 0.01$ vs Bor/C6-M, $n = 4$, data are shown in mean ± SD. (C) Relative uptake of micelles after pretreatment with different inhibitors. $^{**}P < 0.01$, $n = 4$, data are shown in mean ± SD. (D) Cell apoptosis induced by different formulations. $^{**}P < 0.01$ vs CMS; $^{\#}P < 0.05$ vs Bor/CMS-M, $^{\#\#}P < 0.01$ vs Bor/CMS-M, $n = 4$, data are shown in mean ± SD.

2.3 Influence of micelles on brain microvascular endothelial cells

We evaluated the effects of various micelles on the proliferation, cellular uptake, cell membrane integrity, and permeability of endothelial cells. As shown in Figure 3A, CMS-M inhibited the proliferation of HBMEC cells by 45% with concentrations higher

 doi:10.20944/preprints201810.0574.v1

than 2 μg/mL, which was significantly higher than Bor/CMS-M and Pep-1/Bor/CMS-M groups. The Pep-1 modification has little effect on toxicity toward HBMEC, suggesting that Bor may be helpful to reducing the cytotoxicity of micelles against endothelial cells through increasing bi-directional permeability of the cell membrane. C6 was used as a fluorescent probe to evaluate the uptake of different micelles by HBMEC cells. As shown in Figure 3B, Bor/C6-M and Pep-1/Bor/C6-M showed significantly higher endocytosis by HBMEC cells than the C6-M group, suggesting that borneol modification was of great importance to improve cellular uptake [24]. However, the modification of Pep-1 exhibited no obvious effect on endothelial cell uptake, probably because of a low expression of the IL-13 receptor on the surface of HBMEC cells. To explore the effect of micelles on the integrity of the tight junction, we also tested the changes of TEER after incubation of different micelles with endothelial cells. As shown in Figure 3C, there were no significant changes in TEER values of HBMEC cells after 4 h of treatment with CMS-M. However, both Bor/C6-M and Pep-1/Bor/C6-M decreased TEER values significantly after incubation for 15 min. With extended times, the TEER value continued to decrease until 120 min, suggesting that borneol modification could reduce the integrity of the junction between endothelial cells, thereby facilitating the entry of particles into the BBB, which is consistent with previous reports about the ability of borneol to facilitate delivery into the brain [25]. Finally, we evaluated the effects of different functional groups on the permeability of endothelial cells. As shown in Figure 3D, the Papp of CMS-M reached a plateau within 1 h (approximately 4.5×10^7 cm/s) and remained relatively stable over further 3 h. In contrast, Bor/C6-M and Pep-1/Bor/C6-M reached their maximum potential within 2 h (about 7.8×10^7 cm/s), which was significantly higher than that of CMS-M, suggesting that borneol modification is more effective for BBB penetration [14]. As expected, no significant difference was observed between Bor/C6-M and Pep-1/Bor/C6-M, suggesting that the main contribution of Pep-1 is to recognize tumor cells and enhance internalization, and that of borneol is to enhance the ability to penetrate the BBB and to enhance the uptake by tumor cells to some extent.

Preprints (www.preprints.org) | NOT PEER-REVIEWED | Posted: 24 October 2018 doi:10.20944/preprints201810.0574.v1

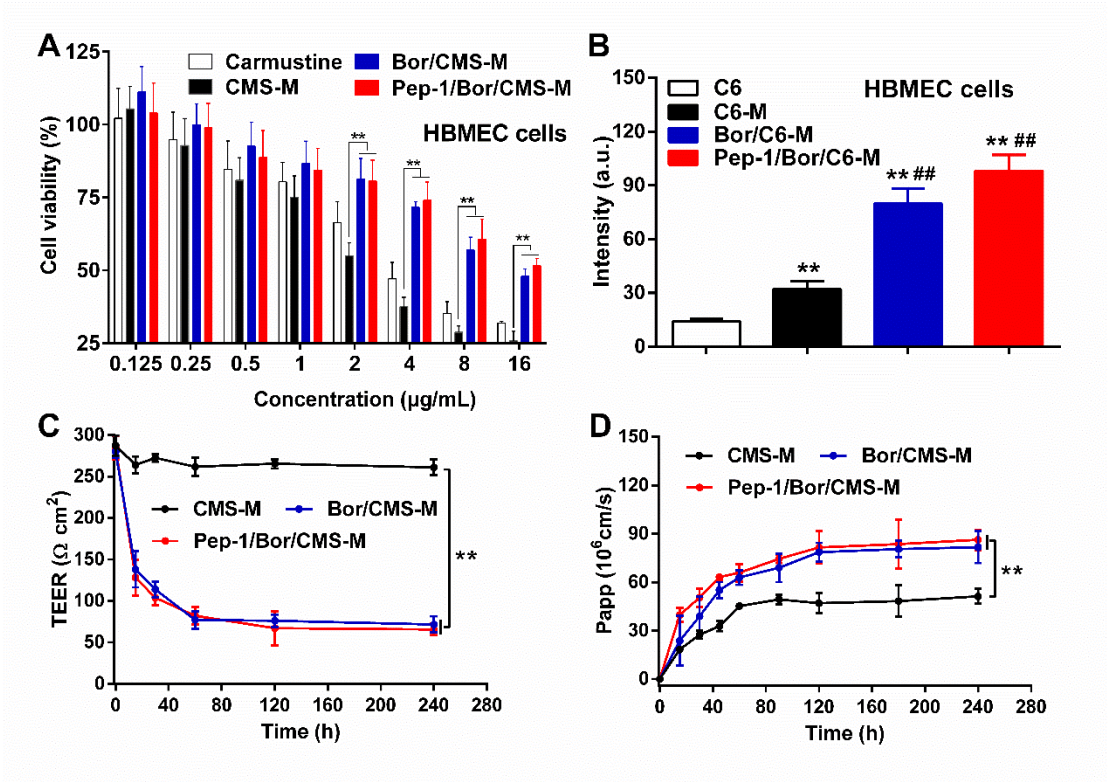

Figure 3. Influence of micelles on HBMEC cells. (A) Antiproliferative effect of different micelles against HBMEC cells. $^{**}P < 0.01$, n = 6, data are shown in mean ± SD. (B) Cellular uptake of micelles on HBMEC cells. $^{**}P < 0.01$ vs C6, $^{\#\#}P < 0.01$ vs C6-M, n = 4, data are shown in mean ± SD. (C) Alternations of TEER after treatment with different micelles. $^{**}P < 0.01$, n = 3, data are shown in mean ± SD. (D) Changes of Papp after treatment with different micelles within 240 min.$^{**}P < 0.01$, n = 3, data are shown in mean ± SD.

2.4 In vivo *imaging*

Brain targeting and prolonged retention were the key objectives in designing Pep-1/Bor/CMS-M. DiD was used as a near-infrared probe to evaluate the biodistribution of the different micelles. As shown in Figure 4A, due to the enhanced permeability and retention (EPR) effect, DiD/M displayed a relative better brain-targeted ability than DiD at 6 h post-injection, but the fluorescence eliminated rapidly. Single-administrated DiD/Bor/M significantly increased the signal distribution at the brain tissues, suggesting that borneol modification enhanced the ability to penetrate the BBB, however, the fluorescence in the brain obviously decreased after 6 h. Most importantly, DiD/Pep-1/Bor/M displayed an overwhelming brain-targeted ability, indicating that simultaneous modification of Pep-1 and Bor was indeed capable of carrying sufficient

Preprints (www.preprints.org) | NOT PEER-REVIEWED | Posted: 24 October 2018 doi:10.20944/preprints201810.0574.v1

CMS into the glioma sites via borneol-based BBB-penetration enhancement and Pep-1-based active tumor/brain targeting. Notably, the signal was still observed at 24 h post treatment, suggesting a prolonged retention at the desired sites and thereby of the potential toxic-reduced effects [20]. We also quantified the fluorescence in brain sites at 6 h and 24 h post-injection. As shown in Figure 4B, the fluorescence intensity of the three micelle groups had better brain targeting than free DiD at different observation time intervals. DiD/Bor/M and DiD/Pep-1/Bor/M groups was significantly higher than that of the DiD/M. As expected, DiD/Pep-1/Bor/M exhibited the highest accumulation and the longest retention at the brain sites, confirming the advantages of the dual-functional modification of borneol and Pep-1 in targeted therapy.

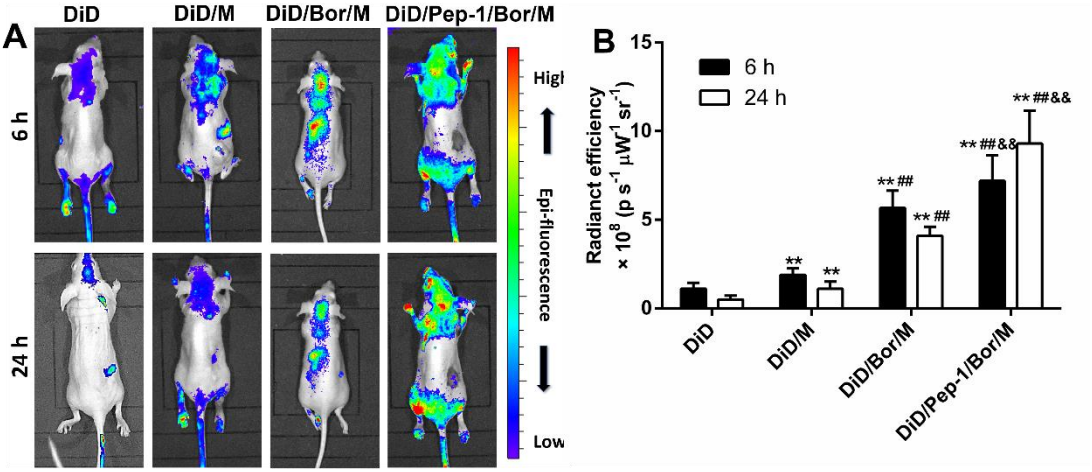

Figure 4. Biodistribution in orthotopic Luc-BT325 glioma tumor-bearing nude mice. (A) Biodistribution of fluorescence signal after single administration of different DiD-labelled formulations at 6 h and 24 h post injection. (B) ROI quantitation of fluorescence of brain site at 6 h and 24 h post treatment. $^{**}P < 0.01$ vs DiD at the corresponding time; $^{\#\#}P < 0.01$ vs DiD/M at the corresponding time; $^{\&\&}P < 0.01$ vs DiD/Bor/M at the corresponding time. n = 3; Data represented as mean ± SD.

2.5 In vivo *anticancer efficacy*

We have validated that Pep-1/Bor/CMS-M can efficiently penetrate HBMEC cells and strongly kill BT325 cells *in vitro*. In this part, the effects of the micelles on inhibition of tumor growth, and survival period were investigated using orthotopic Luc-BT325 glioma tumor-bearing nude mouse models with interval administration. As

 doi:10.20944/preprints201810.0574.v1

shown in Figure 5A, all treatments significantly inhibited tumor growth. Specifically, three types of micelles retarded the growth of tumors more severely than CMS, which might be related to a prolonged retention time *in vivo* and an enhanced stability of CMS caused by micellular encapsulation [26]. As we expected, Bor/CMS-M displayed a higher antitumor effect than CMS-M, that was attributed to the enhanced accumulation in brain tissues. Most importantly, the signal at the tumor of mice treated with Pep-1/Bor/CMS-M was the weakest at day 28, suggesting the strongest antitumor efficacy among all treatments. It reflected the importance and significance of combinational modification with Pep-1 and Bor in micelles in the targeted treatment of glioma. In order to quantify the tumor inhibition, the relative photo flux calculated as the ratio of luminescence at day 28 to that at day 14 was plotted in Figure 5B. Similarly, the relative photo flux of mice treated with Pep-1/Bor/CMS-M was the lowest among all the treatments, further validating the feasibility and rationality of our design. Figure 5C shows the survival period of nude mice treated with various formulations. All animals died at day 45 in the Carmustine-treated group. Due to micelle-endowed toxicity reduction and increase in tumoral uptake, the survival period of mice treated with CMS-M was prolonged to 49 days. The maximum survival time of mice treated with Bor/CMS-M reached 53 days, probably attributed to the enhanced penetration to BBB. Notably, 25 % of Pep-1/Bor/CMS-M-treated mice still survived at day 53, which was significantly better than other groups. Overall, the survival time was positively correlated with the ability of tumor inhibition.

Preprints (www.preprints.org) | NOT PEER-REVIEWED | Posted: 24 October 2018 doi:10.20944/preprints201810.0574.v1

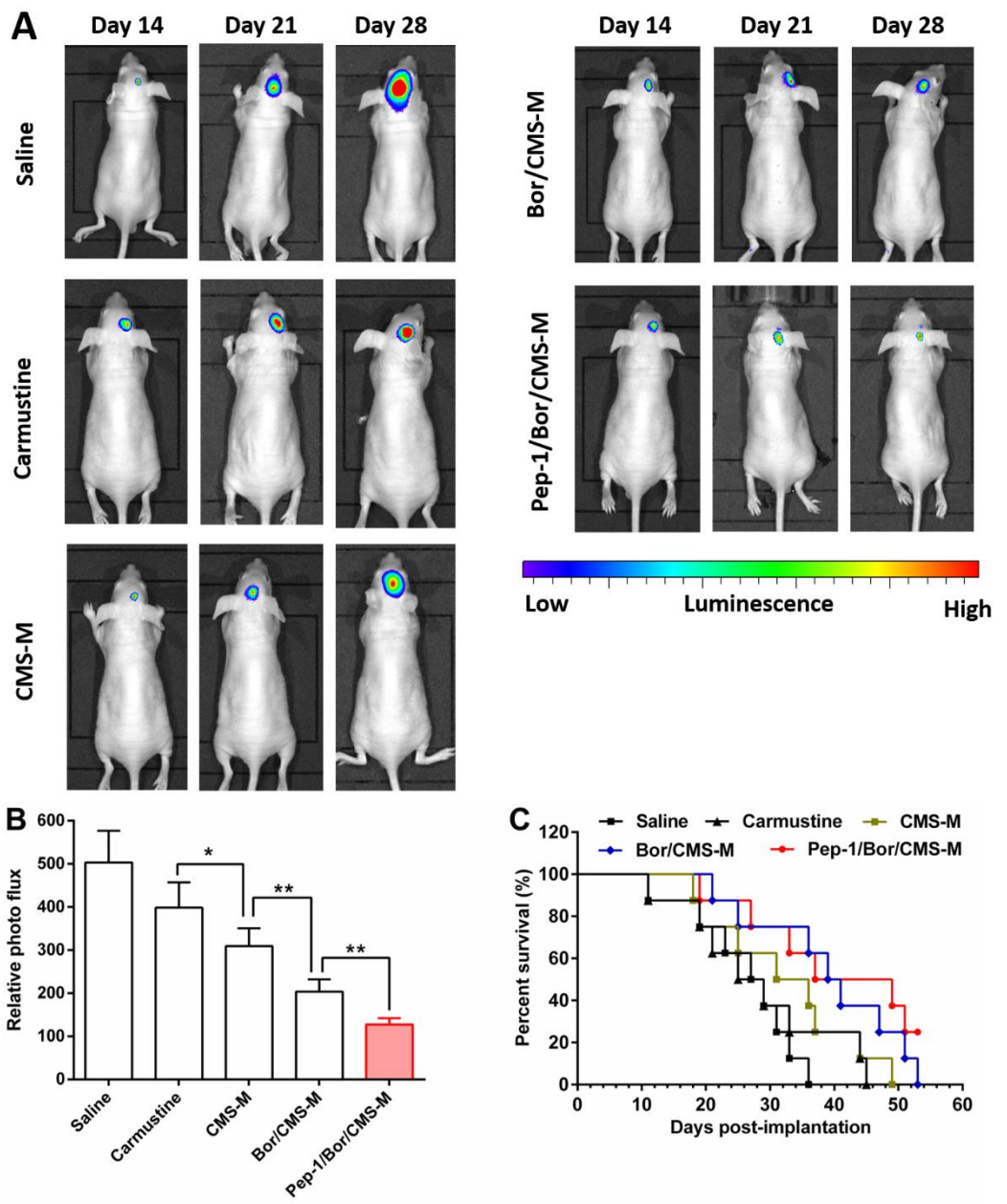

Figure 5. In vivo anticancer efficacy. (A) Bioluminescence of tumors of orthotopic Luc-BT325 glioma tumor-bearing nude mice treated with different formulations at d 14, d 21 and d 28 post implantation. (B) The ratio of photo flux at d 14 to that at d 28 at the brain of mice treated with different formulations. $^{**}P < 0.01$, n = 6. (C) Survival period of mice treated with different formulations within 53 days.

2.6 In vivo *Safety evaluation*

Body weight loss, damage of normal organs and abnormal in biochemical assay occurred commonly during the clinical application of CMS [27]. As shown in Figure 6A, Pep-1/Bor/CMS-M did not lead to the significant decrease of body weight after six

Preprints (www.preprints.org) | NOT PEER-REVIEWED | Posted: 24 October 2018 doi:10.20944/preprints201810.0574.v1

injections. Likewise, no obvious difference was found in the spleen/liver index of mice treated with different carmustine formulations after 48 h of the last administration. As shown in Figure 6C to 6D, the liver and kidney function did not alter obviously. These results suggested that Pep-1/Bor/CMS-M enabled anticancer treatment be relatively safe at such determined dose.

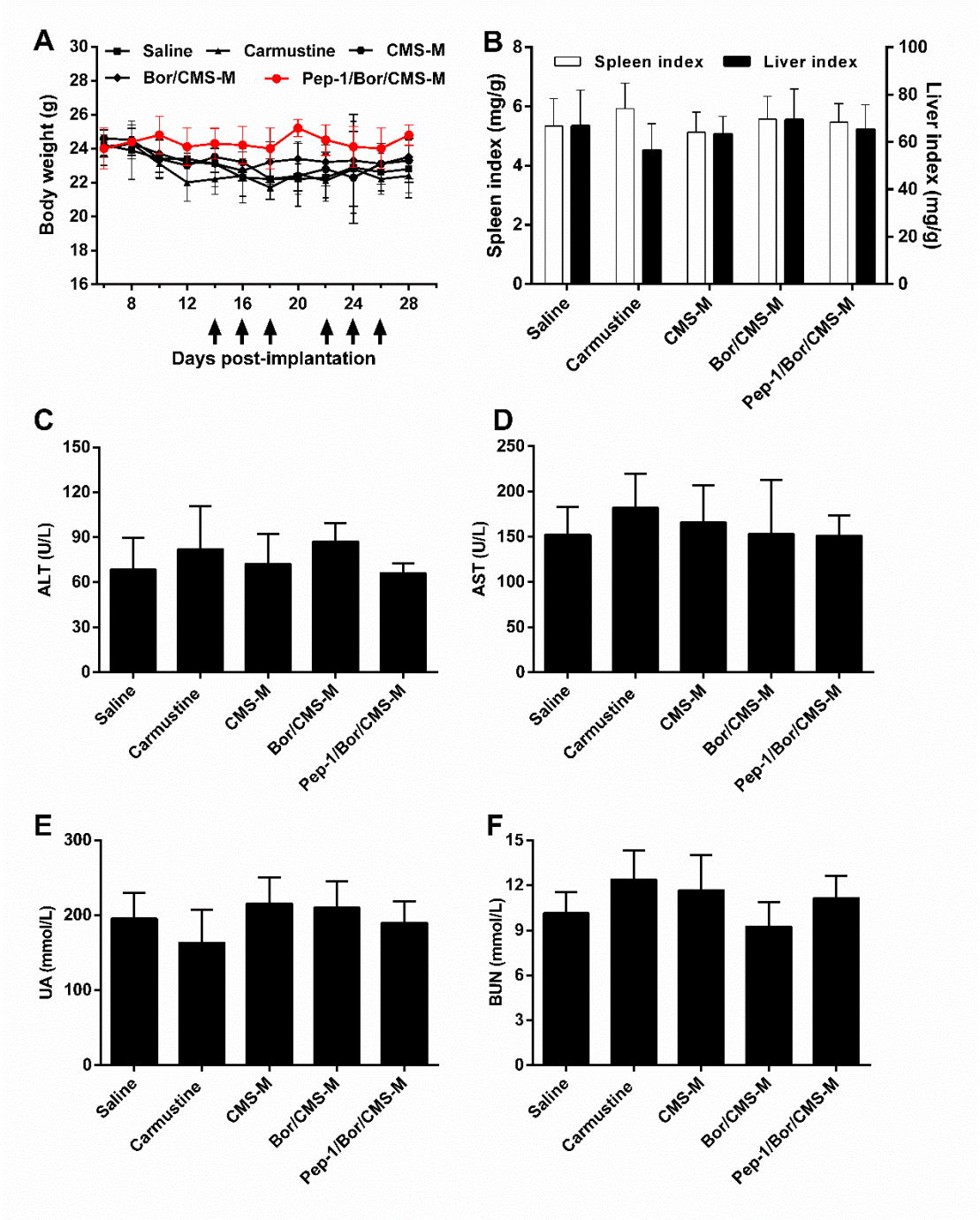

Figure 6. In vivo safety evaluation. (A) Changes in body weight of mice treated with different formulations during the period of the observation. n = 6. The arrows represent the administration

Preprints (www.preprints.org) | NOT PEER-REVIEWED | Posted: 24 October 2018 doi:10.20944/preprints201810.0574.v1

time. (B) The ratio of the weight of liver/spleen to the body at the end of the observation. n = 6. Concentration of (C) ALT, (D) AST, (E) UA and (F) BUN in serum of mice treated with various formulations. n = 6.

3. Materials and methods

3.1 Materials

CMS (purity > 99%) was purchased from Nanjing Axiannu BioTech Co., Ltd. (Nanjing, China); Pep-1 peptide, DSPE-PEG-Pep-1 and DSPE-PEG-Bor were synthesized by GL BioTech Co., Ltd. (Shanghai, China), the chemical structures of the latter two lipids were showed in Figure S2; DOPE was purchased from A.V.T Co., Ltd. (Shanghai, China). Amiloride, sucrose and genistein were provided by Sinopharm Chemical Reagent Co., Ltd. (Shanghai, China); Coumarin 6 (C6) and 1,1'-Dioctadecyl-3,3,3',3'-tetramethylindo dicarbocyanineperchlorate (DiD) were provided by Aladdin Chemical Co., Ltd. (Shanghai, China). Human interleukin 13 (IL-13) ELISA Kit was obtained from Abcam trading company Ltd. (Shanghai, , China). Fetal bovine serum (FBS) and tetramethylazole salt (MTT) were purchased from Thermo Fisher BioTech Co., Ltd. (MA, USA); RPMI 1640 medium, DMEM medium, trypsin and dimethyl sulfoxide (DMSO) were bought from GIBCO BioTech Co., Ltd. (Thermo Fisher Scitific, MA, USA).

3.2 Preparation and characterization of micelles

2.5 mg of DSPE-PEG-Pep-1, 5 mg of DSPE-PEG-Bor, 25 mg of DSPE-PEG, 17.5 mg of DOPE and 2 mg of CMS were simultaneously dissolved in 100 mL of methanol, following by rapid injection into 2 mL of deionized water under the vigorous stirring [28,29]. After 5 min of stirring, micelle was loaded into a dialysis bag with a cut-off molecular weight of 3000, and then dialyzed against flowing water for 6 h at room temperature to obtain Pep-1/Bor/CMS-M. CMS-M was prepared by the similar method by replacing DSPE-PEG-Bor and DSPE-PEG-Pep-1 with the same amount of DSPE-PEG. Similarly, Bor/CMS-M was prepared by the similar method by replacing DSPE-PEG-Pep-1 with the same amount of DSPE-PEG. C6-labelled Pep-1/Bor-M (Pep-

Preprints (www.preprints.org) | NOT PEER-REVIEWED | Posted: 24 October 2018 doi:10.20944/preprints201810.0574.v1

1/Bor/C6-M) was prepared by the similar method except that replacement of CMS with 0.1% (wt%) of C6. DiD-labelled Pep-1/Bor-M (DiD/Pep-1/Bor/M) was prepared by the similar method except that replacement of CMS with 0.05% (wt%) of DiD. Micelles prepared above were filtered by 0.22 microporous membrane, following by determination of particle size, polydisperse index (PDI) and zeta potential by dynamic light scatter (DLS, Malvern Company, UK) at a total concentration of 3 mg/mL. The micellar filtrate was 10 fold-diluted by methanol and then quantified by HPLC (Agilent 1260, USA). After lyophilization, the powder of micelle was dissolved in 2 mL deionized water, the drug within that was determined by the similar method. Encapsulation efficiency (%) = drug in micelle/feeding drug × 100%; drug loading (%) = drug in freeze-dried powder/freeze-dried powder × 100%.

3.3 Morphological observation

10 μL of Pep-1/Bor/CMS-M solution at a total concentration of 30 mg/mL was dropped onto a TEM exclusively-used copper mesh. After air-drying, the sample was stained with 10 μL of 1% phosphotungstic acid for 5 sec, followed by drying under infrared lamp and observing by Transmission Electron Microscope (TEM, Tecnai 12, Philiips, Netherlands) immediately.

3.4 Drug release

1.0 mL of Pep-1/Bor/CMS-M solution containing 1 mg of CMS was loaded in a dialysis bag with a cut-off molecular weight of 3000, and then immersed in 100 mL of phosphate buffer (pH 7.4~5.0) with 0.5% (V%) of Tween 80, respectively. The samples were rotated in a dissolution apparatus (YiChen Instrument Co., Ltd, Shanghai, China) at a rate of 60 r/min. At the predetermined time intervals, 0.5 mL of medium were withdrew with complement of equivalent corresponding fresh medium. After demulsification with 9-fold methanol and centrifugation at 13000 r/min for 10 min, the drug content was determined by HPLC. Likewise, the drug release behavior of Bor/CMS-M and CMS-M in pH 7.4 medium was also determined by the similar method. The formula of drug release is calculated as follows. Release percentage (%) = $(1-C_t \times 1 \times 10/C_0 \times 1) \times 100\%$, where C_t and C_0 represent the CMS concentration of samples and

Preprints (www.preprints.org) | NOT PEER-REVIEWED | Posted: 24 October 2018 doi:10.20944/preprints201810.0574.v1

the initial CMS concentration of samples, respectively.

3.5 Cytotoxicity

Cell culture: Human glioma BT325 cells and luciferase-labelled BT325 (Luc-BT325) cells were cultured with RPMI1640 containing 10% FBS, and human brain microvascular endothelial cells (HBMECs) were cultured in the DMEM medium containing 20% FBS and 100 μg/mL endothelial cell growth factor. 100 μg/mL of penicillin-streptomycin solution was added to according mediums if necessary. Two kinds of cell lines were incubated in incubator (HERAcell 2401, Thermo Fisher, USA) at 37°C and 5%CO_2 atmosphere. The culture medium was changed every other day. The cells were passaged using trypsin when the coverage reached 70% ~ 80%.

MTT assay: BT325 cells at logarithmic growth stage were cultured in 96-well culture plate with 200 μL each well. After 24 h of incubation, the culture medium was replaced with 200 μL of CMS, CMS-M, Bor/CMS-M and Pep-1/Bor/CMS-M at a CMS concentration ranging from 0.125 to 16 μg/mL. After 24 hours of culture, 10 μL of MTT solution (5 mg/mL) was mixed with medium for 4 h, following by removing the mixture and adding 160 μL of DMSO into each well. The absorbance at 492 nm was detected by a multimode plate reader (Multiskan FC, Thermo Fisher, USA). The cell viability was calculated as follows, cell viability (%) = absorbance of test group/ absorbance of control group × 100%. Likewise, the cytotoxicity of micelles against HBMEC cells were investigated as the similar method.

3.6 Cellular uptake

2×10^4 of BT325 cells were inoculated in 24-well culture plate. When reached 80% of confluence, the cells were washed with PBS thrice and treated with C6, C6-M, Bor/C6-M and Pp-1/Bor/C6-M at a C6 concentration of 50 ng/mL for 4 h. At the end of this time, the cells were washed with PBS thrice and added with trypsin to prepare cell suspension. Finally, the suspension containing 5000 cells was immediately tested by a flow cytometry (C6 plus, BD, USA). Likewise, the internalization of micelles by HBMEC cells were studied by the similar method.

3.7 Mechanism of endocytosis

Preprints (www.preprints.org) | NOT PEER-REVIEWED | Posted: 24 October 2018 doi:10.20944/preprints201810.0574.v1

2×10^4 of BT325 cells were inoculated in 24-well culture plate. When reached 80% of confluence, the cells were washed with PBS thrice and pretreated with sucrose (0.4 μM), amiloride (0.4 nM), genistein (0.2 nM) and IL-13 (50 ng/mL) for 30 min, respectively [30]. PBS was here used as a negative control of inhibitors. Next, the cells were incubated with C6-M, Bor/C6-M and Pp-1/Bor/C6-M at a C6 concentration of 50 ng/mL in the presence of various inhibitors above-mentioned. After 4 h of treatment, the cells were washed with PBS thrice and added with trypsin to prepare cell suspension. Finally, the suspension containing 5000 cells was immediately tested by a flow cytometry (C6 plus, BD, USA). The relative uptake was calculated as the following formulas, relative uptake rate (%) = intensity of samples/intensity of control × 100%.

3.8 Cell apoptosis

400 μL of BT325 cell suspension containing 4×10^5 cells were inoculated into 24-well culture plate. After culture for 24 h, the cells were treated with CMS, CMS-M, Bor/CMS-M, Pep-1/Bor/CMS-M (2 μg/mL of CMS), and PBS was used as control group. After 6 h of incubation, the culture medium was removed, followed by washing with 400 μL of ice PBS thrice, and adding 100 μL of trypsin to the well. And then, 100 μL of cell suspension was stained with 100 μL of Annexin V-PE assay kit (Guava, Merck-Millipore, Germany) in dark. After 15 min of incubation, the samples were immediately analyzed by flow cytometry.

3.9 In vitro *penetration of micelles*

As reported previously [14], 1×10^5 cells of HBMEC cells were seeded into Transwell® insert with a pore size of 3 μm (Corning, USA) for 96 h. When the transepithelial electrical resistance (TEER) value was higher than 250 Ωcm^2, in vitro BBB model was considered as successful establishment. Next, 200 μL of CMS-M, Bor/CMS-M and Pep-1/Bor/CMS-M containing 0.5 μg/mL of CMS were added into the upper compartments. At the predetermined intervals, 200 μL of medium was withdraw from the lower compartments, followed by complement with equivalent fresh medium. The TEER was measured with a transepithelial electrical resistance instrument (Millicell-ERS-2, Millipore). The Apparent permeability coefficient (Papp)

Preprints (www.preprints.org) | NOT PEER-REVIEWED | Posted: 24 October 2018 doi:10.20944/preprints201810.0574.v1

was calculated as follows, Papp = dQ/dt/SC, where dQ/dt represents the transport ratio, S represents the area of membrane, and C represents the initial concentration of CMS.

3.10 Orthotopic glioma model

One microliter of cell suspension containing 2×10^5 Luc-BT325 cells was slowly implanted into the right corpus striatum of BALB/C (nu/nu) nude mice (2.1 mm lateral to bregma and 3 mm in depth) under the online-anesthetization by isoflurane [15, 21]. Prior to observation of the growth of tumors, the mice were firstly treated with D-luciferin potassium (as a luciferase substrate) at a dose of 80 mg/kg and then monitored the luminescence by in vivo imaging system (IVIS Lumina II, Xenogen, USA) equipped with a bioluminescence detector [31].

3.11 In vivo *imaging*

Twelve orthotopic Luc-BT325 glioma tumor-bearing nude mice were randomly divided into four groups and intravenously administrated with DiD, DiD/M, DiD/Bor/M and DiD/Pep-1/Bor/M at a DiD dose of 400 ng/kg, respectively. At 6 h and 24 h post injection, the mice were placed under the near-infrared imaging system to acquire the biodistribution of fluorescence signal at excitation of 640 nm and emission of 710 nm. At 24 h post administration, the tumor-bearing brain tissues were harvested, followed by quantifying the intensity by using the region of interest (ROI) tool.

3.12 In vivo *anticancer efficacy*

Sixty orthotopic Luc-BT325 glioma tumor-bearing nude mice were randomly divided into five groups: Saline, CMS, CMS-M, Bor/CMS-M and Pep-1/Bor/CMS-M. (Study approval number RCX (Su)-20161028). Each of mice was intravenously administrated 0.2 mL of formulation at a CMS dose of 2 mg/kg. During and after the treatment, the body weight of mice was measured, and the luminescence of tumor were monitored by the imaging system. After 48 h of the last administration, 6 mice were randomly selected from each group for the observation of survival period, and the rest was sacrificed to collect liver, spleen and prepare the serum samples for the detection of liver/spleen index and biochemical assay [32]. The liver/spleen index was calculated by the weight of liver/spleen to the weight of body weight. The biochemical assay of

 doi:10.20944/preprints201810.0574.v1

serum samples, including alanine aminotransferase (ALT), aspertate aminotransferase (AST), uric acid (UA) and blood urine nitrogen (BUN) were performed according to the corresponding standard protocols.

3.13 Data statistics

The data are expressed as mean ± SD, and processed by SPSS16.0 software. $P < 0.05$ represents significant difference and $P < 0.01$ means extremely significant difference. Students' two-tail *t* test is employed for statistics comparisons.

4. Conclusions

In this study, we developed a carmustine-based micelle delivery system capable of promoting BBB permeation and targeting glioma through the bifunctional modification of Bor and Pep-1. Pep-1/Bor/CMS-M was prepared simply, and its morphological behavior was not affected by various functional modifications. The micelle can not only increase the cellular uptake and cytotoxicity against BT325 cells, but also improve the permeability into HBMEC cells through reducing the tight junction. In orthotopic Luc-BT325 glioma tumor-bearing nude mice models, Pep-1/Bor/CMS-M enhanced the targeted accumulation, improved the brain retention, inhibited the tumor growth and prolonged the survival period. This study brings a novel concept for the glioma-targeted treatment.

Funding: This work was supported by Nanjing Medical Science and technology development Foundation (grant number YKK16275).

Acknowledgment

We acknowledge the financial support from Nanjing Medical Science and technology development Foundation (grant number YKK16275).

Declaration of interest: The authors have no potential conflicts of interest in this work.

References

1 Akilo, O.D.; Choonara, Y.E.; Strydom, A.M.; du Toit, L.C.; Kumar, P.; Modi, G.; Pillay, V. AN in vitro evaluation of a carmustine-loaded Nano-co-Plex for potential magnetic-targeted intranasal delivery to the brain. *Int. J. Pharm.* **2016**, *500*, 196-209.

2 Brandes, A.A.; Bartolotti, M.; Tosoni, A.; Franceschi, E. Nitrosoureas in the management of malignant gliomas. *Curr. Neurol. Neurosci. Rep*. **2016**, *16*, 13.

3 Ohue, S.; Kohno, S.; Inoue, A.; Yamashita, D.; Suehiro, S.; Seno, T.; Kumon, Y.; Kikuchi, K.; Ohnishi, T. Evaluation of serial changes on computed tomography and magnetic resonance imaging after implantation of carmustine wafers in patients with malignant gliomas for differential diagnosis of tumor recurrence. *J. Neurooncol.* **2016**, *126*, 119-126.

4 Lee, J.S.; An, T.K.; Chae, G.S.; Jeong, J.K.; Cho, S.H.; Lee, H.B.; Khang, G. Evaluation of in vitro and in vivo antitumor activity of BCNU-loaded PLGA wafer against 9L gliosarcoma. *Eur. J. Pharm. Biopharm*. **2005**, *59*, 169-175.

5 Akiyama, Y.; Kimura, Y.; Enatsu, R.; Mikami, T.; Wanibuchi, M.; Mikuni, N. Advantages and disadvantages of combined chemotherapy with carmustine wafer and bevacizumab in patients with newly diagnosed glioblastoma: A single-institutional experience. *World Neurosurg.* **2018**, *113*, e508-e514.

6 Kim, J.H.; Kim, Y.; Bae, K.H.; Park, T.G.; Lee, J.H.; Park, K. Tumor-targeted delivery of paclitaxel using low density lipoprotein-mimetic solid lipid nanoparticles. *Mol. Pharm*. **2015**, *12*, 1230-1241.

7 Qu, D.; Lin, H.; Zhang, N.; Xue, J.; Zhang, C. In vitro evaluation on novel modified chitosan for targeted antitumor drug delivery. *Carbohydr. Polym.* **2016**, *92(1)*, 545-54.

8 Nakamura, I.; Ichimura, E.; Goda, R.; Hayashi, H.; Mashiba, H.; Nagai, D.; Yokoyama, H.; Onda, T.; Masuda, A. An in vivo mechanism for the reduced peripheral neurotoxicity of NK105: a paclitaxel-incorporating polymeric micellar nanoparticle formulation. *Int. J. Nanomedicine* **2017**, *12*, 1293-1304.

9 Sonali; Agrawal, P.; Singh, R.P.; Rajesh, C.V.; Singh, S.; Vijayakumar, M.R.; Pandey, B.L.; Muthu, M.S. Transferrin receptor-targeted vitamin E TPGS micelles for brain

cancer therapy: preparation, characterization and brain distribution in rats. *Drug Deliv.* **2015**, *2*, 1-11.

10 Xu, C.F.; Liu, Y.; Shen, S.; Zhu, Y.H.; Wang, J. Targeting glucose uptake with siRNA-based nanomedicine for cancer therapy. *Biomaterials* **2015**, *51*, 1-11.

11 Alyautdin, R.; Khalin, I.; Nafeeza, M.I.; Haron, M.H.; Kuznetsov, D. Nanoscale drug delivery systems and the blood-brain barrier. *Int. J. Nanomedicine* **2014**, *9*, 795-811.

12 Foley, C.P.; Rubin, D.G.; Santillan, A.; Sondhi, D.; Dyke, J.P.; Crystal, R.G.; Gobin, Y.P.; Ballon, D.J. Intra-arterial delivery of AAV vectors to the mouse brain after mannitol mediated blood brain barrier disruption. *J. Control. Release* **2014**, *196*, 71-78.

13 Huang, P.; Jiang, X.F.; Zou, J.L.; Yuan, Y.M.; Yao, M.C.; Lu, Y.S. A novel GC–MS bioanalytical method for natural borneol and its application in investigating natural borneol distribution in mice mode. *Tradit. Chin. Med. Mater. Med*. **2009**, *11*, 821-827.

14 Song, H.; Wei, M.; Zhang, N.; Li, H.; Tan, X.; Zhang, Y.; Zheng, W. Enhanced permeability of blood-brain barrier and targeting function of brain via borneol-modified chemically solid lipid nanoparticle. *Int. J. Nanomedicine* **2018**, *13*, 1869-1879.

15 Ruan, S.B.; Qin, L.; Xiao, W.; Hu, C.; Zhou, Y.; Wang, R.; Sun, X.; Yu, W.Q.; He, Q.; Gao, H.L. Acid‐Responsive Transferrin Dissociation and GLUT Mediated Exocytosis for Increased Blood–Brain Barrier Transcytosis and Programmed Glioma Targeting Delivery. *Adv. Funct. Mater*. **2018**, *28(30)*, 1802227.

16 Freije, W.A.; Castro-Vargas, F.E.; Fang, Z.; Horvath, S.; Cloughesy, T.; Liau, L.M.; Mischel, P.S.; Nelson, S.F. Gene expression profiling of gliomas strongly predicts survival. *Cancer Res.***2004**, *64*, 6503-6510.

17 Garcia, C.R.; Slone, S.A.; Pittman, T.; St Clair, W.H.; Lightner, D.D.; Villano, J.L. Comprehensive evaluation of treatment and outcomes of low-grade diffuse gliomas. *PLoS One* **2018**, *13*, e0203639.

18 Wu, A.; Ericson, K.; Chao, W.; Low, W.C. NFAT and AP1 are essential for the expression of a glioblastoma multiforme related IL-13Ra2 transcript. *Cell Oncol.* **2010**, *2*, 313-329.

19 Debinski, W.; Gibo, D.M.; Slagle, B.; Powers, S.K.; Gillespie, G.Y. Receptor for interleukin 13 is abundantly and specifically over-expressed in patients with glioblastoma multiforme. *Int. J. Oncol*. **1999**, *15*, 481-486.

20 Wang, X.; Zhang, Q.; Lv, L.; Fu, J.; Jiang, Y.; Xin, H.; Yao, Q. Glioma and microenvironment dual targeted nanocarrier for improved anti glioblastoma efficacy. *Drug Deliv.* **2017**, *24*, 1401-1409.

21 Gao, H.; Yang, Z.; Zhang, S.; Cao, S.; Pang, Z.; Yang, X.; Jiang, X. Glioma-homing peptide with a cell-penetrating effect for targeting delivery with enhanced glioma localization, penetration and suppression of glioma growth. *J. Control. Release* **2013**, *172(3)*, 921-8.

22 Kim, H.K.; Thompson, D.H.; Jang, H.S.; Chung, Y.J.; Van den Bossche, J. pH-responsive biodegradable assemblies containing tunable phenyl-substituted vinyl ethers for use as efficient gene delivery vehicles. *ACS Appl. Mater. Interfaces*. **2013**, *5*, 5648-5658.

23 Hubčík, L.; Funari, S.S.; Pullmannová, P.; Devínsky, F.; Uhríková, D. Stimuli responsive polymorphism of C12NO/DOPE/DNA complexes: Effect of pH, temperature and composition. *Biochim. Biophys. Acta* **2015**, *1848*, 1127-1138.

24 Hu, L.; Chen, D.Y. Application of headspace solid phase microextraction for study of noncovalent interaction of borneol with human serum albumin. *Acta Pharmacol. Sin*. **2009**, *30*, 1573–1576.

25 Zhao, J.Y.; Lu, Y.; Du, S.Y.; Song, X.; Bai, J.; Wang, Y. Comparative pharmacokinetic studies of borneol in mouse plasma and brain by different administrations. *J. Zhejiang Univ. Sci. B.* **2012**, *13*, 990–6.

26 Cabral, H.; Kataoka, K. Progress of drug-loaded polymeric micelles into clinical studies. *J. Control. Release* **2014**, *190*, 465-476.

27 Scott, A.W.; Tyler, B.M.; Masi, B.C.; Upadhyay, U.M.; Patta, Y.R.; Grossman, R.; Basaldella, L.; Langer, R.S.; Brem, H.; Cima, M.J. Intracranial microcapsule drug delivery device for the treatment of an experimental gliosarcoma model. *Biomaterials* **2011**, *32(10)*, 2532-9.

28 Wu, H.; Zhu, L.; Torchilin, V.P. pH-sensitive poly(histidine)-PEG/DSPE-PEG co-polymer micelles for cytosolic drug delivery. *Biomaterials* **2013**, *34*,1213-22.

29 Li, X.; Dong, Q.; Yan, Z.; Lu, W.; Feng, L.; Xie, C.; Xie, Z.; Su, B.; Liu, M. MPEG-DSPE polymeric micelle for translymphatic chemotherapy of lymph node metastasis. *Int. J. Pharm.* **2015**, *487*, 8-16.

30 Su, X.; Gao, C.; Shi, F.; Feng, X.; Liu, L.; Qu, D.; Wang, C. A microemulsion co-loaded with Schizandrin A-docetaxel enhances esophageal carcinoma treatment through overcoming multidrug resistance. *Drug Deliv.* **2017**, *24*, 10-19.

31 Zou, Y.; Liu, Y.; Yang, Z.; Zhang, D.; Lu, Y.; Zheng, M.; Xue, X.; Geng, J.; Chung, R.; Shi B. Effective and Targeted Human Orthotopic Glioblastoma Xenograft Therapy via a Multifunctional Biomimetic Nanomedicine. *Adv. Mater.* **2018**, 1803717.

32 Hsu, C.Y.; Yang, C.F.; Liao, L.R.; Ho, H.L.; Ho, D.M. Tonsil surface epithelium is ideal for monitoring Ki-67 immunohistochemical staining. *Histopathology* **2013**, *63*, 810-816.